8-1-2017

Chasing Boundaries and Cascade Effects in a Coupled Barrier-Marsh-Lagoon System

Jorge Lorenzo Trueba
Montclair State University, lorenzotruej@mail.montclair.edu

Giulio Mariotti
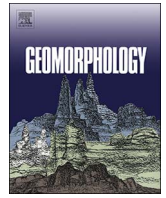*Louisiana State University*

Chasing boundaries and cascade effects in a coupled barrier-marsh-lagoon system

Jorge Lorenzo-Trueba[a,*], Giulio Mariotti[b,c]

[a] Department of Earth and Environmental Studies, Montclair State University, NJ 07043, USA
[b] Department of Oceanography and Coastal Sciences, Louisiana State University, Baton Rouge, LA 70803, USA
[c] Center for Computation and Technology, Louisiana State University, Baton Rouge, LA 70803, USA

ABSTRACT

The long-term dynamic evolution of an idealized barrier-marsh-lagoon system experiencing sea-level rise is studied by coupling two existing numerical models. The barrier model accounts for the interaction between shoreface dynamics and overwash flux, which allows the occurrence of barrier drowning. The marsh-lagoon model includes both a backbarrier marsh and an interior marsh, and accounts for the modification of the wave regime associated with changes in lagoon width and depth. Overwash, the key process that connects the barrier shoreface with the marsh-lagoon ecosystems, is formulated to account for the role of the backbarrier marsh. Model results show that a number of factors that are not typically associated with the dynamics of coastal barriers can enhance the rate of overwash-driven landward migration by increasing backbarrier accommodation space. For instance, lagoon deepening could be triggered by marsh edge retreat and consequent export of fine sediment via tidal dispersion, as well as by an expansion of inland marshes and consequent increase in accommodation space to be filled in with sediment. A deeper lagoon results in a larger fraction of sediment overwash being subaqueous, which coupled with a slow shoreface response sending sediment onshore can trigger barrier drowning. We therefore conclude that the supply of fine sediments to the back-barrier and the dynamics of both the interior and backbarrier marsh can be essential for maintaining the barrier system under elevated rates of sea-level rise. Our results highlight the importance of considering barriers and their associated backbarriers as part of an integrated system in which sediment is exchanged.

1. Introduction

Low-lying coasts are often characterized by barrier islands, km-wide stretches of sand separated from the mainland by marshes and lagoons. Barriers commonly serve as buffer zones between the coastal ocean and mainland human population centers and infrastructure, protecting these communities from the most devastating coastal impacts of climate change. Barriers themselves are also some of the most popular tourist and recreational destinations in the US, and constitute some of the most valuable real estate in the country (Heinz-Center, 2000; Morton, 2008). Furthermore, barriers support biodiversity (McLachlan, 1983), provide a range of ecosystem services (Barbier et al., 2010), and protect wetlands that, in turn, support their own diverse ecologies (Day et al., 2008).

Despite the economic and ecological importance of barriers, and their extensive presence along the US East and Gulf coasts, there exists a critical gap in understanding how barrier systems respond to coastal change. In particular, there is a poor understanding of the complex

barrier-backbarrier interactions, which results in landward migration rates unprecedented in thousands of years (FitzGerald et al., 2008). In order to fill this gap we build an exploratory numerical model (Murray, 2003) to examine the morphological feedbacks within a barrier-marsh-lagoon system and predict its evolution under projected rates of sea-level rise and sediment supply to the backbarrier environment.

Our starting point is a recently developed morphodynamic model (Lorenzo-Trueba and Ashton, 2014) that couples shoreface evolution and overwash processes in a dynamic framework. As such, the model is able to capture dynamics not reproduced by morphokinematic models, which advect geometries without specific concern to processes. These dynamics include periodic barrier retreat due to time lags in the shoreface response to barrier overwash, height drowning due to insufficient overwash flux as sea level rises, and width drowning, which occurs when the shoreface response rate is insufficient to maintain the barrier geometry during overwash-driven landward migration. The model, however, does not incorporate dynamic processes landward of the barrier, such as erosion and accumulation of

---

peat and lagoonal sediments, which influence the space available for sediment to accumulate behind the barrier and hence control the island migration rate that is triggered by sea-level rise (Bruun, 1988).

The two-way interactions between backbarrier marsh and barrier have been recently explored with GEOMBEST + (Walters et al., 2014; Brenner et al., 2015), a modified version of the GEOMBEST model (Stolper et al., 2005; Moore et al., 2010). The study highlighted how the backbarrier marsh can slow down the island migration rate by reducing the space available for sediment to fill, and that overwash facilitates the persistence of a stable backbarrier marsh. Additionally, coupling field observations with GEOMBEST + suggests that sediment overwash allows a narrow marsh to be maintained in a long-lasting alternate state within a range of conditions under which they would otherwise disappear (Walters et al., 2014). Here we propose to further investigate the evolution of barrier and backbarrier environments by coupling a morphodynamic barrier model (Lorenzo-Trueba and Ashton, 2014) with a dynamic model for the evolution of the marsh platform and the marsh boundary with the adjacent lagoon. In particular, we have extended a model developed by Mariotti and Carr (2014) to include both a backbarrier and an interior marsh, and modified the barrier overwash flux to account for the presence of a backbarrier marsh. The resulting model represents a cross-section that spans from the toe of the shoreface to the point where the marshes encroach the mainland, that is, the upper limit of the marine influence (Fig. 1). This modeling framework allows us to explore new feedbacks between barrier and their backbarrier ecosystems that have not been tackled before.

2. Coupled model description

Our model approach assumes an idealized cross-section (Fig. 1) that connects the shoreface, the barrier, and the backbarrier. The backbarrier, defined here as the region between the barrier and the upper limit of the marine influence, includes three units: a backbarrier marsh (or rear fringing marsh), a lagoon, and an inland marsh. The barrier model component accounts for the interaction between shoreface dynamics and overwash flux, and the marsh-lagoon component explicitly describes marsh edge processes of both the backbarrier marsh and the interior marsh, and accounts for the modification of the wave regime associated with lagoon width, which coincides with the wave fetch.

2.1. Barrier dynamics

Our model focuses on two primary barrier system components or behavioral elements: the marine domain represented by the active shoreface, and the backbarrier environment, where the infrequent process of overwash controls landward mass fluxes. As described in Lorenzo-Trueba and Ashton (2014), the evolution of the barrier system can be fully determined with the rates of migration of the shoreface toe $\dot{x}_T = dx_T/dt$, the shoreline $\dot{x}_S = dx_S/dt$, the landward end of the subaerial portion of the barrier $\dot{x}_B = dx_B/dt$, and the change of the barrier height $\dot{H} = dH/dt$ (Fig. 1). These rates can be written in terms of the sediment flux at the shoreface Q_{SF}, the sea-level rise rate $\dot{z}$, the total overwash flux Q_{OW}, the top-barrier overwash component $Q_{OW,H}$ and the backbarrier overwash component $Q_{OW,Bm}$ (Figs. 1 and 3):

$$\dot{x}_T = 4Q_{SF}\frac{H + D_T}{D_T(2H + D_T)} + \frac{2\dot{z}}{\alpha} \tag{1}$$

$$\dot{x}_S = \frac{2Q_{OW}}{2H + D_T} - 4Q_{SF}\frac{H + D_T}{(2H + D_T)^2} \tag{2}$$
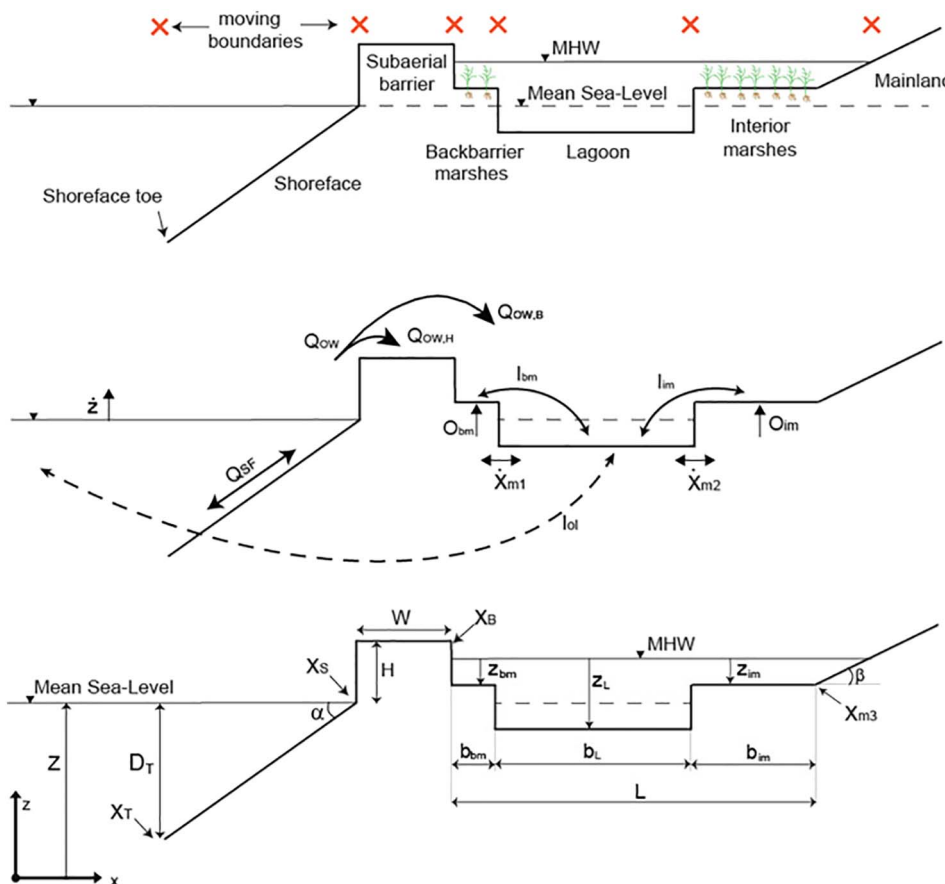
Fig. 1. Cross-shore barrier-marsh-lagoon-marsh-mainland model set up, including (a) the different geomorphic domains and their moving boundaries, (b) key processes that drive the evolution of the moving boundaries, (c) state variables. This is the general cross-section of the system, but note that the model can also account for scenarios in which backbarrier and/or inland marshes completely disappear (i.e., $b_{bm} = 0$ and/or $b_{im} = 0$).
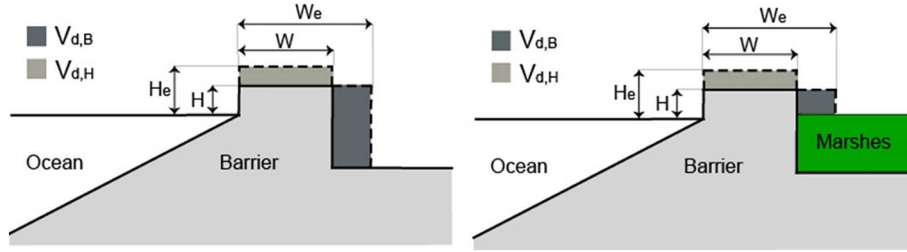
Fig. 2. Schematic of the critical barrier island width concept and the top-barrier $V_{d,H}$ and back-barrier $V_{d,B}$ deficit volumes. Note that when backbarrier accommodation is filled by marshes, $V_{d,B}$ is reduced.

$$\dot{x}_B = \frac{Q_{OW,Bm}}{H + z_{bm} - r/2} \tag{3}$$

$$\dot{H} = \frac{Q_{OW,H}}{W} - \dot{z} \tag{4}$$

where H is the barrier height, W is the barrier width, α is the shoreface depth, D_T is the shoreface depth, z_{bm} is the backbarrier marsh depth, r is the tidal range, and $\dot{z}$ is the sea-level rise rate (Fig. 1). We compute the shoreface and overwash sediment fluxes following Lorenzo-Trueba and Ashton (2014). Shoreface sediment fluxes are determined based upon deviations from an equilibrium profile. When the shoreface slope is shallower than its equilibrium slope, sediment flux at the shoreface is directed onshore. In contrast, when the shoreface slope is steeper than the equilibrium slope, sediment is directed offshore. Additionally, we compute overwash flux using a simple formulation that relies upon the critical length concept (Leatherman, 1983). This formulation assumes the existence of a critical barrier width W_e and a critical barrier height H_e beyond which overwash flux to the back and the top of the barrier shuts down. When the barrier width W and height H are below their critical values, the overwash rates $Q_{OW,H}$ and $Q_{OW,B}$ scale with their associated deficit volumes, $V_{d,B}$ and $V_{d,H}$ (Fig. 2). Lorenzo-Trueba and Ashton (2014) considered a lagoon in the backbarrier and defined the backbarrier deficit volume as $V_{d,B} = \max[0, (W_e - W)(H + z_L - r/2)]$. Here, in order to account for the presence of a backbarrier marsh, we substitute the lagoon depth with a linear combination of the backbarrier marsh depth z_{bm} and the lagoon depth z_L:

$$V_{d,B} = \max[0, (W_e - W)(H + \varphi(z_{bm} - r/2) + (1 - \varphi)(z_L - r/2)] \tag{5}$$

where:

$$\varphi = \min\left(1, \frac{b_{bm}}{b_{bmc}}\right) \tag{6}$$

This formulation is clarified by considering its two end members. When the backbarrier marsh width, b_{bm}, is larger than the critical barrier marsh width, b_{bmc}, i.e., $\varphi = 1$, overwash sediment is unable to reach the lagoon, and thus, only the backbarrier marsh depth z_{bm} is involved in the deficit volume calculation. In contrast, when the backbarrier marsh disappears, i.e., $\varphi = 0$, only the lagoon depth z_L affects the deficit volume calculation, and the model recovers the formulation introduced by Lorenzo-Trueba and Ashton (2014). Thus, this formulation implies that the presence of marsh ecosystems reduces backbarrier accommodation (Fig. 2), which in turn reduces the backbarrier overwash flux (Bruun, 1988). Additionally, for intermediate values of the backbarrier marsh width (i.e., $0 < \varphi < 1$), the backbarrier deficit volume depends on both the marsh and the lagoon elevations (see Eq. (5)). In this intermediate case, sediment overwash can reach both the backbarrier marsh and the lagoon. Consequently, we extend the overwash formulation presented by Lorenzo-Trueba and Ashton (2014) to account for two backbarrier overwash components: a backbarrier marsh overwash flux $Q_{OW,Bm}$, which contributes to the progradation of the barrier over the backbarrier marsh (Fig. 3), and a lagoon overwash flux $Q_{OW,Bl}$, which contributes to the progradation of the backbarrier marsh (Fig. 3). We compute these fluxes as follows:

$$Q_{OW,Bl} = (1 - \varphi)Q_{OW,B} \tag{7}$$

$$Q_{OW,Bm} = \varphi\, Q_{OW,B} \tag{8}$$

Hence, when the backbarrier marsh is very wide, the overwash flux does not reach the lagoon and thus does not contribute to the progradation of the backbarrier marsh (i.e., $Q_{OW,Bl} = 0$). In contrast, when the backbarrier marsh disappears, the backbarrier overwash flux $Q_{OW,B}$ contributes to the landward migration of the barrier (Fig. 3). Additionally, for intermediate values of the backbarrier marsh width, overwash flux contributes to both the landward migration of the barrier and the backbarrier marsh (Fig. 3). In particular, we note that a narrow marsh will prograde faster than a wider marsh due to a larger overwash sediment input (Eqs. (6) to (8)), which allows for the tendency of a narrow backbarrier marsh to persist. In this way, under the right conditions an equilibrium state for the backbarrier marshes can emerge (see Section 3.2), a dynamic that has been previously described by Walters et al. (2014).

We note that this formulation of overwash deposition is partly constrained by the imposed geometry of the system (Fig. 1), and therefore differs from the one implemented in GEOMBEST + (Walters et al., 2014), in which vertical accretion rates vary with distance from the barrier. However, although this formulation oversimplifies the complex process of barrier overwash, it is consistent with the 'critical barrier width' concept introduced by Leatherman (1983), as well as many subsequent numerical implementations to study the long-term evolution of barriers and the shoreline (Jiménez and Sánchez-Arcilla, 2004; McNamara and Werner, 2008). Additionally, we note that the general model framework is flexible such that it could also incorporate different approaches to computing overwash flux.

2.2. Marsh-lagoon dynamics

The dynamics of the backbarrier environment can be fully described with the rates of change of the depth of the lagoon $\dot{z}_L = dz_L/dt$, backbarrier marsh $\dot{z}_{bm} = dz_{bm}/dt$, and interior marsh $\dot{z}_{im} = dz_{im}/dt$, and the rates of change of the backbarrier marsh edge $\dot{x}_{bm} = dx_{bm}/dt$, interior marsh edge $\dot{x}_{im} = dx_{im}/dt$, and the boundary between the interior marsh and mainland $\dot{x}_{mm} = dx_{mm}/dt$.

The horizontal migration of the two marsh boundaries is controlled by the competition by wave erosion and sediment accretion (Mariotti and Fagherazzi, 2013; Mariotti and Carr, 2014). Thus, both erosion rates E_{bm} and E_{im}, and progradation rates P_{bm} and P_{im}, on each side of the lagoon, depend on the reference wind speed, the width and depth of the lagoon, the depth of the marsh, and the sediment concentration in the lagoon. In addition, the backbarrier marsh receives the overwash flux $Q_{ow,Bl}$, and hence the equations read:

$$\dot{x}_{bm} = P_{bm} - E_{bm} + \frac{Q_{OW,Bl}}{z_L - z_{bm}} \tag{9}$$

$$\dot{x}_{im} = E_{im} - P_{im} \tag{10}$$

The variations in height of the two marshes are controlled by the sea-level rise rate, the organic accretion rates O_{bm} and O_{im}, and the inorganic sediment flux from the lagoon to the backbarrier marsh I_{bm}
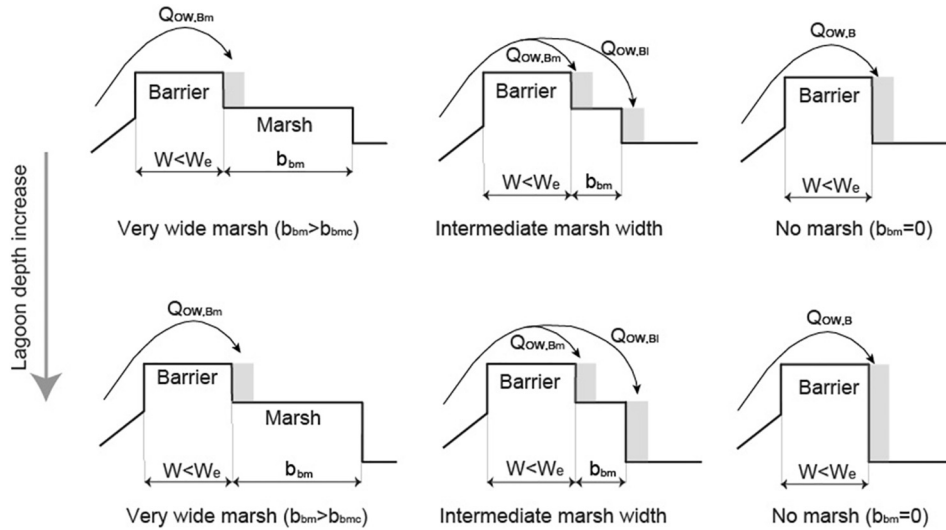
Fig. 3. Schematic of the backbarrier overwash partitioning between the backbarrier face and the marsh.

and the inland marsh I_{im}. I_{bm} and I_{im} are computed through the tidal dispersion mechanism as a function of the reference sediment concentrations in the lagoon and each of the marshes (Mariotti and Carr, 2014):

$$\dot{z}_{bm} = -I_{bm} - O_{bm} + \dot{z} \tag{11}$$

$$\dot{z}_{im} = -I_{im} - O_{im} + \dot{z} \tag{12}$$

Both O_{bm} and O_{im} are assumed to be proportional to refractory component of the annual below ground organic matter production (Mudd et al., 2009; Mariotti and Carr, 2014). Additionally, following Morris et al. (2002), both O_{bm} and O_{im} are computed as a quadratic function of the depth of inundation respect to mean high tide (Morris et al., 2002).

The migration of the inland marsh towards mainland is simply controlled by the height of the interior marsh and the slope of the underlying landscape (Fig. 1):

$$\dot{x}_{mm} = \frac{\dot{z} - \dot{z}_{im}}{\beta} \tag{13}$$

Finally, the variations of the lagoon depth depend on the balance between the horizontal flux at the marsh boundary, the sediment flux from the lagoon to the marsh platform, and the exchange between open ocean and lagoon, I_{ol} (Mariotti and Fagherazzi, 2013; Mariotti and Carr, 2014):

$$\dot{z}_L = I_{bm}\frac{b_{bm}}{b_L} + I_{im}\frac{b_{im}}{b_L} + I_{ol} - (E_{bm} - P_{bm})\frac{z_L - z_{bm}}{b_L} - (E_{im} - P_{im})\frac{z_L - z_{im}}{b_L}$$
$$+ \dot{z} \tag{14}$$

The exchange between lagoon and the open ocean is a key driver of the dynamics of the lagoon, and depends on the balance between sediment export and import. Sediment export is set proportional to the reference sediment concentration in the lagoon C_r, which is determined by wave resuspension. Sediment import is set proportional to the external sediment concentration C_0, (Mariotti and Carr, 2014), which simulates the availability of fine sediment in the nearshore region (Bartholdy and Anthony, 1998; Bartholdy, 2000).

2.3. Model solution

The evolution of the coupled barrier-marsh-lagoon-marsh system is fully determined by the rates of change of the shoreface toe position $\dot{x}_T$, the shoreline position $\dot{x}_S$, the landward end of the subaerial portion of the barrier $\dot{x}_B$, the barrier height $\dot{H}$, the depth of the lagoon $\dot{z}_L$, backbarrier marsh elevation $\dot{z}_{bm}$, interior marsh elevation $\dot{z}_{im}$, the

backbarrier marsh edge $\dot{x}_{bm}$, the interior marsh edge position $\dot{x}_{im}$, and upland marsh edge position $\dot{x}_{mm}$. Combining the barrier and backbarrier processes described in previous section, the evolution of these ten state variables over time is described by Eqs. (1) to (4) and Eqs. (9) to (14).

We numerically solve these equations using a simple Eulerian scheme $\xi = \xi^{old} + \dot{\xi}\Delta t$, where $\xi = x_T, x_S, x_B, H, x_{bm}, x_{im}, x_{mm}, z_{bm}, z_{im}, z_L$. Key input parameter values are listed in Tables 1 and 3; a detailed description of all barrier parameters is included in Lorenzo-Trueba and Ashton (2014), and parameters related to the marsh-lagoon system are included in Mariotti and Carr (2014). As initial barrier geometry (see Fig. 1) we choose:

$$\alpha(t = 0) = \alpha_e,\ W(t = 0) = W_e,\ H(t = 0) = H_e,\ \text{and}\ Z(t = 0) = D_T \tag{15}$$

This initial geometry is at static equilibrium (i.e., $\dot{x}_T = \dot{x}_S = \dot{x}_B = \dot{H} = 0$) for a constant sea level (with corresponding zero shoreface and overwash flux). As initial lagoon, backbarrier marsh and inland marsh widths (see Fig. 1) we choose:

$$b_L(t = 0) = b_{L,0},\ b_{bm}(t = 0) = b_{bm,0},\ b_{im}(t = 0) = b_{im,0} \tag{16}$$

The values for $b_{L,0}, b_{bm,0}$, and $b_{im,0}$ vary between model runs. Their specific values in each figure are included in Table 2. As initial lagoon, backbarrier marsh and inland marsh depths respect to Mean High Water (see Fig. 1) level we choose:

$$z_{bm}(t = 0) = z_{bm,0},\ z_{im}(t = 0) = z_{im,0}\ \text{and}\ z_L(t = 0) = z_{L,0} \tag{17}$$

where $z_{bm,0} = z_{im,0} = 0.26$ m, and $z_{L,0} = 2$ m, which are typical values along the Atlantic and Gulf Coasts.

3. Results

Given that the model has nine dynamic variables (Table 1), explor-

Table 1
Description of key barrier input parameters. A more detailed description of all the parameters related to the barrier system is included in Lorenzo-Trueba and Ashton (2014).

Symbol	Meaning	Units
D_T	Depth of the shoreface toe	L
$\dot{z}$	Relative sea-level rise rate	L/T
W_e	Critical barrier width	L
H_e	Critical barrier height	L
α_e	Shoreface slope at static equilibrium	–
K	Shoreface response rate	$L^3/L/T$
$Q_{OW,\max}$	Maximum overwash sediment flux	$L^3/L/T$
$V_{d,\max}$	Maximum deficit volume	L^3/L

Table 2
Barrier input parameter values used in Figs. 4 to 8.

Figure	D_T (m)	$\dot{z}$ (mm/y)	W_e (m)	H_e (m)	α_e (−)	K (m³/m/y)	$Q_{OW,max}$ (m³/m/y)	$V_{d,max}$ (m³/m)
4	10	5	800	2	0.02	2000	100	$H_e \cdot W_e$
5	10	5	800	2	0.02	2000	100	$H_e \cdot W_e$
6	10	5	800	2	0.02	2000	100	$H_e \cdot W_e$
8	10	*Varies*	800	2	0.02	2000	*Varies*	$H_e \cdot W_e$

Table 3
Description of key backbarrier parameters used in Figs. 4 to 8. A more detailed description of all parameters related to the marsh-lagoon system are included in Mariotti and Carr (2014).

Symbol	Meaning	Units
β	Mainland slope	–
C_0	Sediment concentration in open ocean	L³/L
r	Tidal range	L
P	Tidal period	T
w_s	Settling velocity of lagoon sediment	L/T
U	Wind speed	L/T
B_{peak}	Peak biomass	M/L²
$b_{bm,0}$	Initial backbarrier marsh width	L
$b_{im,0}$	Initial inland marsh width	L
$b_{L,0}$	Initial lagoon width	L
b_{bmc}	Critical backbarrier marsh width	L

ing all the possible combination of parameters and initial conditions is not feasible or useful. In this work, we instead focus on two major aspects that the model is able to capture: the effect of the backbarrier environment (marshes, lagoon, and mainland) on barrier evolution, and the detailed evolution of the backbarrier marsh.

3.1. Effect of marsh-lagoon dynamics on barrier evolution

We first analyze changes in barrier evolution under different lagoon geometries, supply of fine sediment to the backbarrier, as well as different rates of inland marsh expansion towards the mainland. Unless otherwise specified, the parameters for these simulations are given in Table 1.

3.1.1. Lagoon geometry

In order to analyze the effect of lagoon geometry on barrier response, we present two different model runs that only differ in their initial lagoon width (Fig. 4). Additionally, we limit the rate of inland marsh migration towards mainland by imposing a vertical slope at the landward boundary of the basin. In the next section, we relax this condition and explore its effect on the overall behavior.

We first consider the scenario in which $b_{L,0} = 5$ km. As sea level rises and overwash flux activates, the barrier narrows and migrates landwards. The backbarrier marsh shrinks as the rate of barrier migration exceeds the rate of backbarrier marsh expansion on the lagoon side. Both the lagoon width and depth initially increase, indicating that a width of 5 km is above the critical value required for marsh erosion to exceed marsh progradation, and sediment

resuspension in the lagoon to exceed sedimentation (Mariotti and Fagherazzi, 2013). This trend eventually reverses as barrier migration reduces lagoon fetch, which in turn weakens the wind-wave regime, and favors settling of lagoon sediment over resuspension. In this case the import of sediment from the open ocean to the lagoon (the term I_{ol} in Eq. (14)) overwhelms the tendency to export sediment. Additionally, after a response time lag in which shoreface sediment fluxes are directed offshore, onshore sediment fluxes result in barrier widening on the ocean side, which reduces overwash flux and allows even more barrier widening. Despite the changes in the barrier and lagoon geometries, the backbarrier marsh eventually attains a fixed width, which is consistent with the stable narrow state for the backbarrier marsh introduced by Walters et al. (2014).

A larger lagoon width ($b_{L,0} = 30$ km) is associated with larger waves, which cause faster retreat of the inland marsh boundary and larger sediment resuspension in the lagoon. As the concentration of sediment in suspension in the lagoon increases with respect to the sediment concentration in the open sea, sediment export via tidal dispersion is enhanced. Such sediment loss results in more lagoon deepening (increasing accommodation), which increases the fraction of sediment overwash being subaqueous instead of subaerial (Fig. 3). Such a reduction in overwash sediment to the subaerial portion of the barrier, together with shoreface fluxes that are not able to maintain the barrier geometry during such rapid migration, results in barrier drowning. Due to the high supply of overwash sediment, however, the backbarrier marsh is able to keep up with sea-level rise and the fast migration of the barrier before the barrier drowns.

3.1.2. Sediment supply to the lagoon

In this section, we explore how changes in external supply, simulated through the sediment concentration in the open ocean, C_0, can affect barrier response to sea-level rise. To this end, in Fig. 5 we present three different model runs that only differ in their sediment concentration in the open ocean: $C_0 = 0,30,$ and 200 mg/l. These values are in range with field measurements from the Danish Wadden Sea (Bartholdy and Anthony, 1998; Pedersen and Bartholdy, 2006), and with model estimates from Cape May (NJ, USA) (0–20 mg/l) and the Virginia Coastal Reserve (VA, USA) (25–300 mg/l) (Mariotti and Fagherazzi, 2013).

C_0 directly affects the net sediment exchange between the lagoon and the open sea, I_{ol}, which is computed through the tidal dispersion mechanism. With a low external sediment supply ($C_0 = 0$), the export of fine sediment from the lagoon to the open ocean increases, leading to a decline in lagoon sedimentation and lagoon deepening. This increase in backbarrier accommodation results in a larger subaqueous fraction of the storm overwash, which leads to barrier narrowing and faster barrier migration, and an enhancement of the wind-wave regime. The combination of these two factors results in the collapse of both the backbarrier and inland marsh. As the barrier continues its landward migration, however, lagoon fetch and wave energy are reduced. Additionally, as the barrier narrows, overwash flux from the shoreface start to reach the lagoon. This supply of overwash sediment to the backbarrier together with the reduction in wave erosion allow the backbarrier marsh to develop again. Despite the expansion of the backbarrier marsh, however, the shoreface response is not fast enough
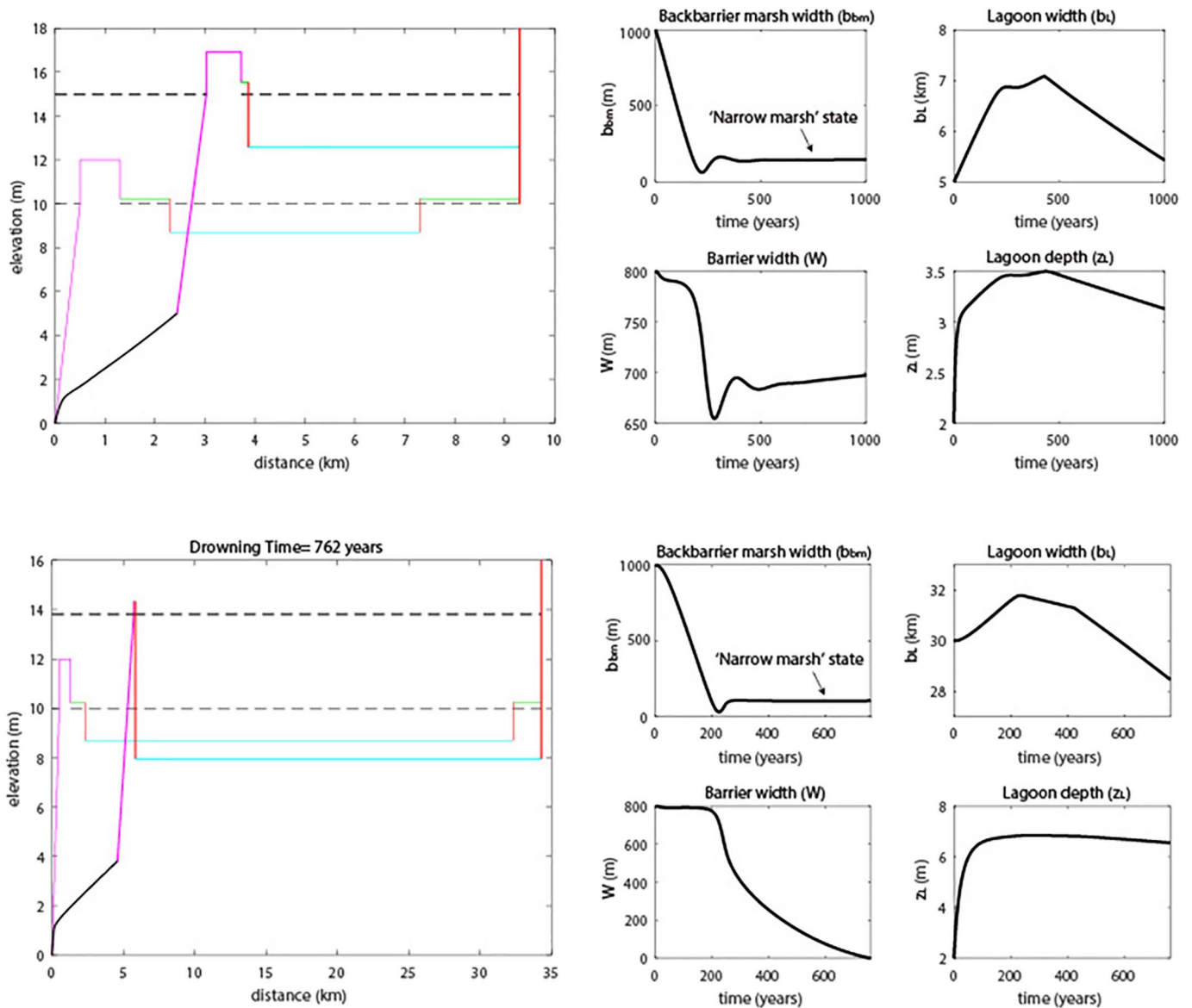
Table 4
Barrier input parameter values used in Figs. 6 to 8.

Figure	$b_{bm,0}$ (km)	$b_{im,0}$ (km)	$b_{L,0}$ (km)	b_{bmc} (km)	β (−)	C_0 (mg/l)	r (m)	P (h)	w_s (mm/s)	U (m/s)	B_{peak} (kg/m²)
4	1	2	*Varies*	1	Vertical	30	1.4	12.5	0.5	10	2.5
5	1	2	10	1	Vertical	*Varies*	1.4	12.5	0.5	10	2.5
6	1	2	20	1	*Varies*	20	2	12.5	0.5	10	2.5
8	1	2	10	1	Vertical	*Varies*	1.4	12.5	0.5	10	2.5

Fig. 4. Profile evolution of modelled barrier-backbarrier systems demonstrating the effect of the initial lagoon width $b_{L,0}$ on barrier response: $b_{L,0} = 5$ km (top), and $b_{L,0} = 30$ km (bottom). Key input parameter values are included in Tables 2 and 4 in the appendix.

to maintain the barrier width and drowning takes place.

An increase in sediment import (e.g., $C_0 = 30$ mg/l) reduces lagoon deepening, and allows the barrier system to keep up with sea-level rise. During its migration the barrier experiences width oscillations due to time lags in the shoreface response, as previously identified in the barrier model (Lorenzo-Trueba and Ashton, 2014). The backbarrier marsh width also fluctuates due to the associated oscillations in overwash flux.

A very large import of sediment to the lagoon (e.g., $C_0 = 200$ mg/l) drastically changes the barrier-backbarrier dynamics. The lagoon depth initially increases, which indicates that the initial lagoon geometry allows sediment resuspension in the lagoon to exceed sedimentation (Mariotti and Fagherazzi, 2013). This trend, however, soon reverses as lagoon sedimentation is favored and lagoon depth starts to decrease. Backbarrier and inland marsh progradation towards the lagoon is also favored, and leads to a reduction in the lagoon width. This reduction in lagoon width weakens the wind-wave regime, which in turn reduces marsh edge erosion. This feedback causes the lagoon to fill in and the barrier to migrate more slowly. These results suggest that processes controlling the dynamics of lagoons, such as external mud supply, play

a strong role on the fate of the barrier island: marsh ecosystems that experience export rather than import of muddy sediments from the open sea are more prone to retreat and drowning.

3.1.3. Rate of inland marsh expansion

The mainland slope β controls the rate at which the inland marsh expands landward. In pristine systems, β is generally very mild, and allows inland marsh migration into the adjacent uplands as sea level rises (Kirwan et al., 2016). However, in many cases marsh migration is constrained by human structures such as seawalls, dykes or revetments (Feagin et al., 2010; Kirwan et al., 2016; Raabe and Stumpf, 2016). To better understand the effect of such constraints on barrier response, we focus on two scenarios. In the first scenario, we prevent marsh expansion towards land by assuming a vertical mainland slope (i.e., $\beta >>>$), which is the same condition that we have used in the previous model runs. In the second scenario, we relax this constraint by assuming a gentle mainland slope (i.e., $\beta = 10^{-4}$).

If marsh expansion towards land is prevented (i.e., $\beta >>>$), the barrier response to sea-level rise and overwash is to narrow and migrate landward. The high rates of marsh erosion initially lead to lagoon
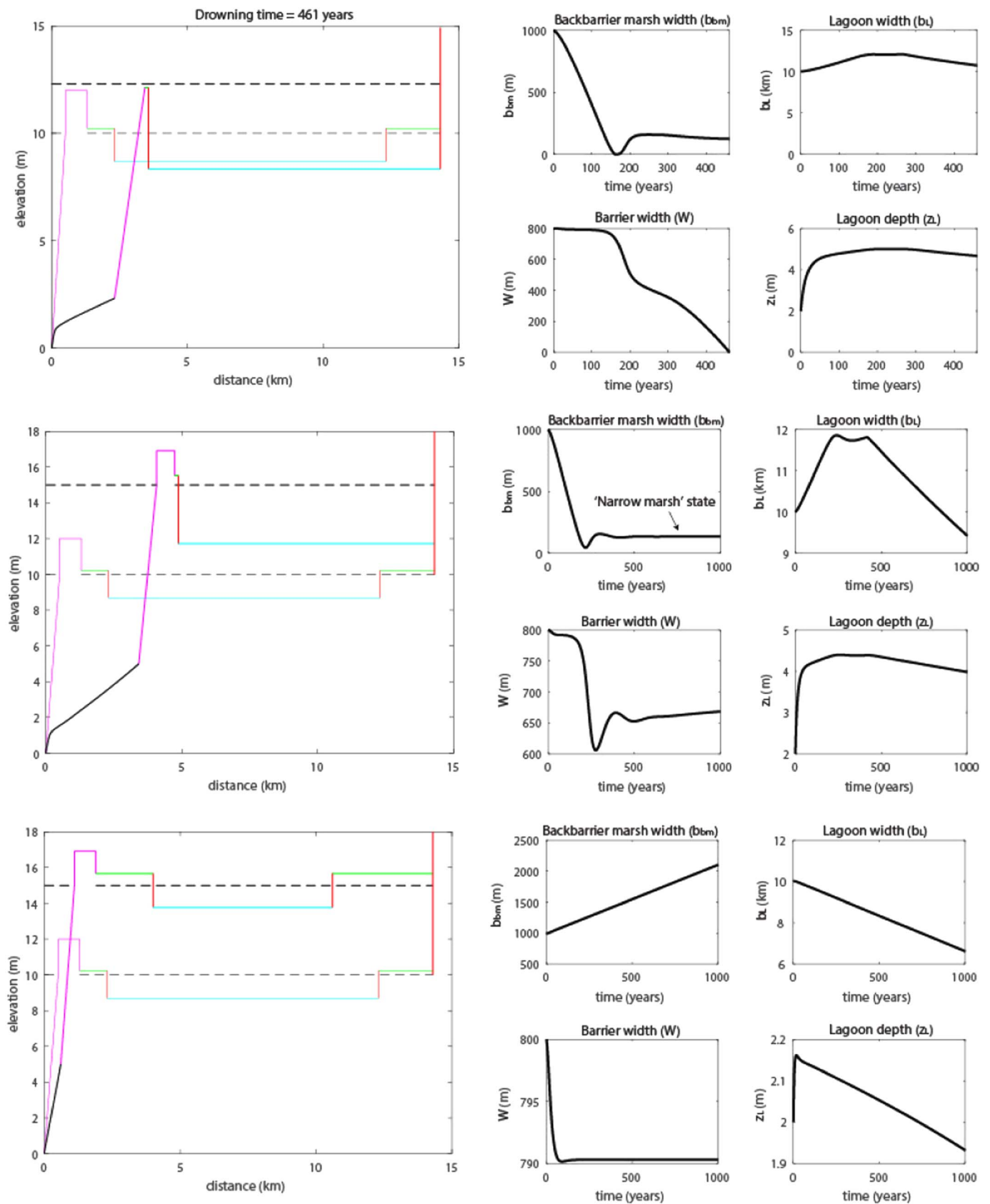
Fig. 5. Profile evolution of modelled barrier-backbarrier systems under different rates of sediment exchange with the open sea: net export of sediments with $C_O = 0$ mg/l (top), mid-scenario with $C_O = 30$ mg/l (center), net import of sediments from the open sea with $C_O = 200$ mg/l (bottom). Key input parameter values are included in Tables 2 and 4 in the appendix.
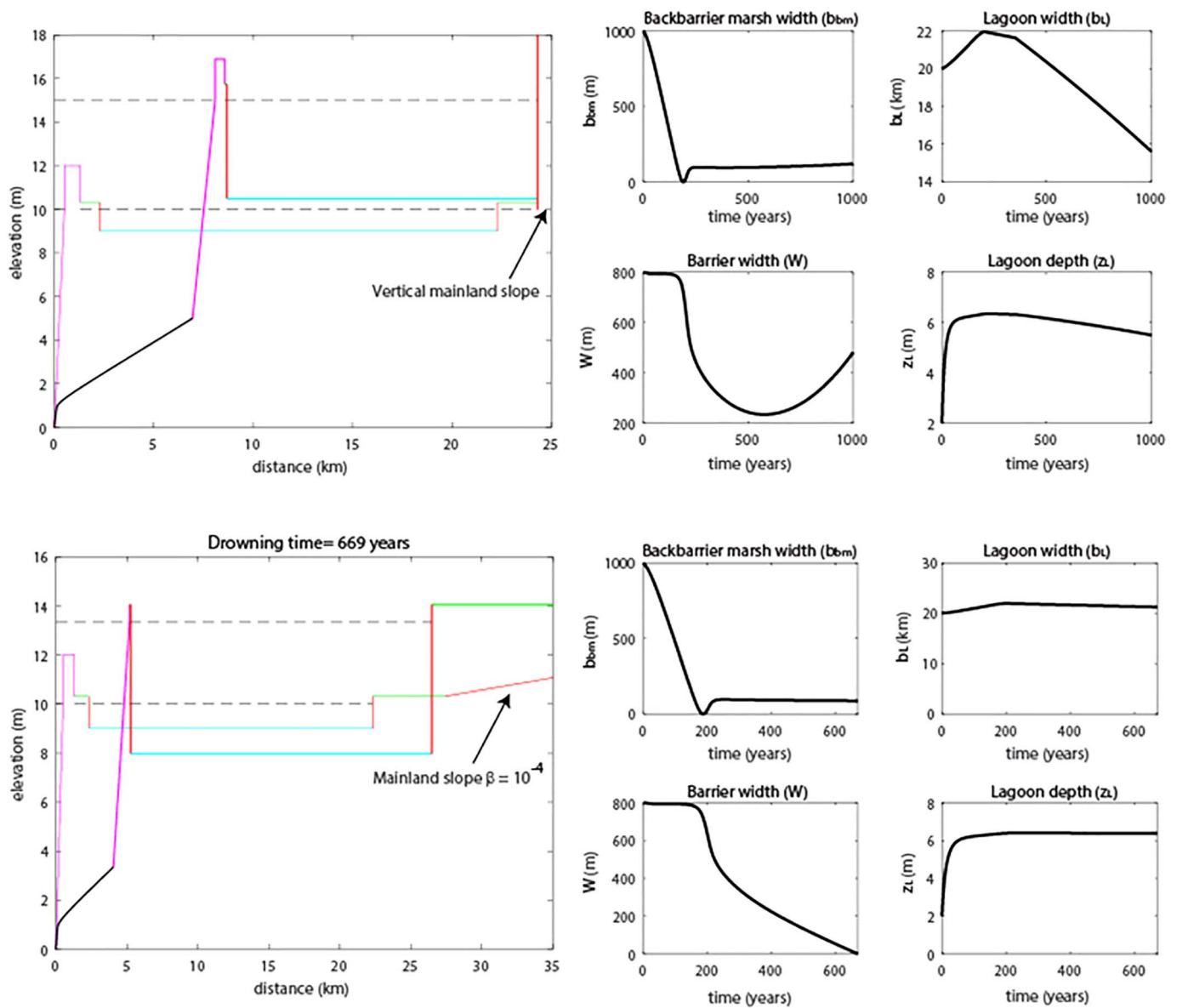
Fig. 6. Profile evolution of modelled barrier-backbarrier systems under two different mainland slopes: $\beta = 10^{-4}$ (top), and $\beta >>>$ (bottom). Key input parameter values are included in Tables 2 and 4 in the appendix.

expansion, which enhances wave activity and triggers lagoon deepening. Eventually, however, marsh erosion diminishes as overwash flux triggers backbarrier marsh progradation. As the landward migration of the barrier continues, this trend reverses and allows onshore sediment fluxes to restore the barrier width.

The dynamics of the lagoon and the barrier changes when the inland marsh is allowed to expand landward (i.e., $\beta = 10^{-4}$). As the inland marsh expands and covers a larger area, it requires a higher supply of sediment from the lagoon, even if the rate of sea-level rise remains constant. The inland marsh effectively becomes a sink of lagoon sediment, the consequence of which is a deepening of the lagoon. Under these conditions, a larger overwash flux is required to fill an increasing backbarrier accommodation space, which leads to fast barrier migration and eventually barrier drowning if the onshore directed fluxes are insufficient. The landward migration of the inland marsh could therefore, through a cascade of effects, trigger barrier drowning.

3.2. Backbarrier marsh dynamics

Changes in the width and height of the backbarrier marsh are driven by processes from both the ocean and the lagoon sides (Fig. 7). Storm-driven overwash from the ocean side typically results in backbarrier marsh expansion towards the lagoon (Eq. (9)) (Walters et al., 2014; Walters and Kirwan, 2016), but it can also bury the portion of the marsh closer to the island, which results in the migration of the landward end of the barrier onto the marsh (Eq. (3)). Wind waves in the lagoon are important drivers of marsh retreat, whereas accumulation of lagoon sediments in front of the marsh leads to marsh progradation towards the lagoon (Mariotti and Fagherazzi, 2013). In this section, we explore the different parameters that control these processes and therefore determine the evolution of the backbarrier marsh.

Sea-level rise rate and external sediment concentration are key factors determining whether the backbarrier marsh drowns, expands, contracts, attains a constant width, or squeezes (Fig. 8a). Marsh
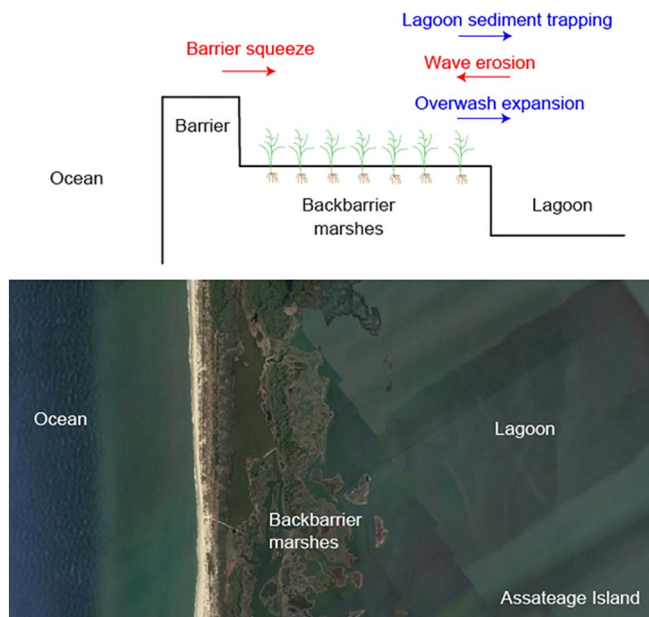
Fig. 7. The top schematic includes the key processes that control the dynamics of backbarrier marshes. Processes that drive marsh contraction are in red, and those that drive marsh expansion in blue. The bottom photograph of Assateague island, Virginia, illustrate the different environments included in the sketch above. (For interpretation of the references to colour in this figure legend, the reader is referred to the web version of this article.)

drowning occurs under high rates of sea-level rise and low lagoon sediment concentrations. Under these conditions, the feedback between flooding duration and reduced organic matter accumulation eventually results in marsh being unable to vertically keep up with sea-level rise (Morris et al., 2002). Marsh expansion often occurs under low sea-level rise rates and high lagoon sediment concentrations, although sediment input from rivers can also be an important contributor (Vogel et al., 1996). In these circumstances, the backbarrier marsh tends to prograde into the lagoon, which reduces backbarrier accommodation space and lowers the rate of barrier migration (Fig. 3). When the rate of marsh progradation exceeds the rate of barrier migration, the width of the marsh increases (Fig. 8c). In contrast, when the barrier retreats faster than the rate of marsh progradation towards the lagoon, the marsh undergoes width contraction. Because the overwash flux to the marsh edge increases as the marsh width decreases (Fig. 3), marsh contraction could halt when the marsh becomes very narrow, and an equilibrium condition in which marsh edge progradation balances barrier migration is attained (Fig. 8c). If the marsh progradation rate, even with the aid of the overwash flux, is smaller than the barrier migration rate, then the marsh contracts and eventually disappears. If the marsh edge retreats instead of prograding, then the marsh is squeezed from both ends: the barrier side and the lagoon side. This condition, which we define as "barrier squeeze" (Fig. 8b, d), is the most deleterious, and leads to the fastest rate of marsh loss.

These results emphasize how overwash flux can be essential to explain changes in the width of the backbarrier marsh. In particular, overwash flux plays a dominant role under low lagoon sediment concentrations, when barrier migration rates and erosion by locally-generated waves are typically high. Under these conditions, a reduction in the maximum overwash flux results in the squeeze of the backbarrier marsh until its eventual disappearance (Fig. 8d). These results support recent work suggesting that overwash flux provides an essential supply of inorganic sediment, which allows a minimum backbarrier marsh width to be maintained under high rates of sea-level rise (Rodriguez et al., 2013; Walters et al., 2014).

4. Discussion and implications

Model results presented in this manuscript are not intended to specifically reproduce the evolution of any particular coastal system but to reveal the coupling between the barrier and its backbarrier environments. This approach implies that processes that could affect the response of the coupled system are purposely omitted from this version of the model. For instance, the model presented here assumes that the barrier is composed of uniform grain-size and non-cohesive sediment. The effect of non-sandy lithology outcrops at the shoreface, however, can also alter the response of the coupled system (Brenner et al., 2015). In particular, muddy sediments deposited in the backbarrier environment that will later outcrop on the shoreface do not contribute to the sand volume as the barrier migrates landwards. As discussed by Brenner et al. (2015), such reduction in coarse sediment maintaining the barrier could significantly enhance barrier drowning.

The model does not account for changes in backbarrier hypsometry, which can affect the sediment dispersal along the barrier complex (Georgiou et al., 2005). Additionally, inland and backbarrier marsh environments are characterized with an average elevation with respect to mean sea level, which does not allow for the presence of different plant species. Future modeling efforts will aim to dynamically account for the long-term evolution of both low and high marshes in the backbarrier environment.

Furthermore, the model does not incorporate the effect of along-shore gradients, spit formation, barrier breaching and inlet closure, or ebb and flood tidal delta sediment dynamics. Current modeling efforts, however, aim at incorporating these effects. In particular, the barrier model component has recently been extended to account for both the alongshore and cross-shore transport directions (Ashton and Lorenzo-Trueba, 2015).

Leaving out many of the processes operating in a complex system such as a barrier-marsh-lagoon environment can potentially increase the clarity and insights the model facilitates (Murray, 2003), and therefore highlight the importance of considering barriers and their associated backbarriers as part of an integrated system in which sediment is exchanged. In particular, model results demonstrate that factors such as lagoon geometry, export of fine sediments from the lagoon to the open ocean, and the slope of mainland, which are typically not directly related to barrier evolution, could play a major effect on the long-term barrier response to sea-level rise. Moreover, model results presented here suggest that the supply of sediments (particularly muddy sediment) to the lagoon can not only help repair marsh environments, but also slow down the rate of barrier migration and potentially reduce the risk of future barrier drowning. Future modeling efforts will span a wider range of scenarios and parameter values to explore whether an increase in sediment supply in the backbarrier has always the same effect.

This coupled system approach is particularly important when seeking to maximize the resilience of coastal communities to predicted increases in storm intensity (Emanuel, 2013), and a rising mean sea level (IPCC, 2014), which increases the impact of storm events (Tebaldi et al., 2012). Yet, restoration activities often follow a compartmental approach, where the focus is limited to a very small part of a large system. For example, marsh restoration activities, such as de-embankment of previously reclaimed salt-marsh land, opening anthropogenic dikes, (re)creating tidal channels, vegetating intertidal dredge disposal, nutrient flux modifications, and hardening marsh shorelines to prevent marsh edge erosion (Weinstein et al., 2001; Teal and Weishar, 2005; Wolters et al., 2005), generally do not account for their consequences on barrier islands. Additionally, billions of dollars are spent on barrier stabilization efforts such as beach nourishment practices, jetties, groins, or sea walls (Titus et al., 1991; NAP, 1995; Trembanis et al., 1999). Such barrier stabilization efforts may serve to protect vulnerable barrier communities, but are commonly undertaken without full understanding of the potential impacts on associated backbarrier ecosystems. For
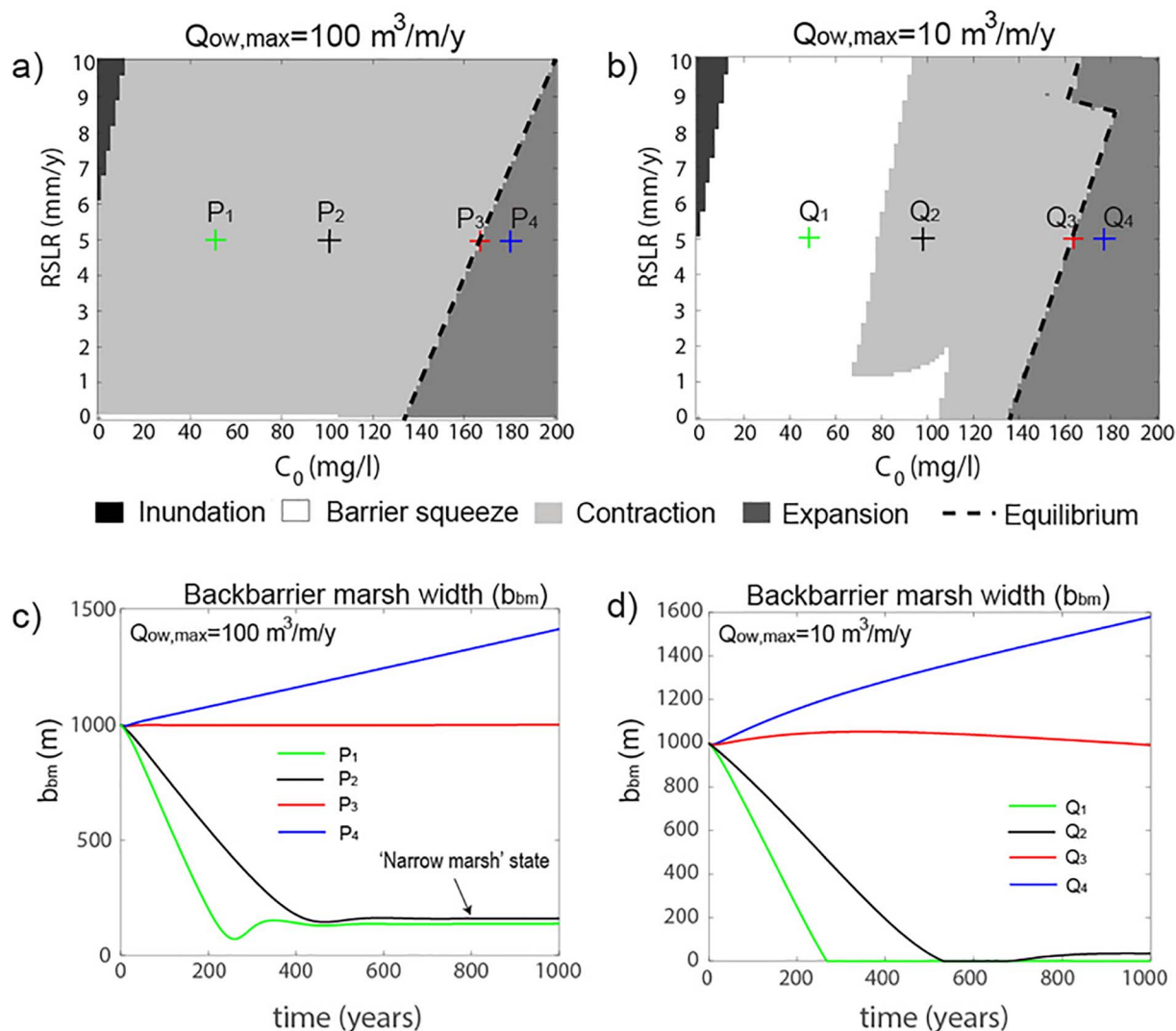
Fig. 8. Regime diagrams including different system behaviors as sea-level rise rate and the external sediment concentration are varied. The only difference between the two regime diagrams is the maximum overwash flux: (a) $Q_{ow,max} = 100$ m³/m/y and (b) $Q_{ow,max} = 10$ m³/m/y. (c) and (d) depicts the barrier width over time for four different cases in the regime diagrams as indicated. Key input parameter values are included in Tables 2 and 4 in the appendix.

instance, anthropogenic structures on barrier islands can limit the landward extent and volume of overwash deposition relative to a nearby natural area (Rogers et al., 2015). This reduction of inorganic sediment supply to the backbarrier marsh can, in turn, diminish backbarrier marsh resilience to wave erosion (Fig. 8).

Acknowledgements

References

Ashton, A.B., Lorenzo-Trueba, J., 2015. Complex responses of barriers to sea-level rise emerging from a model of alongshored-coupled dynamic profile evolution. In: Coastal Sediments San Diego, USA, .

Barbier, E.B., Hacker, S.D., Kennedy, C., Koch, E.W., Stier, A.C., Silliman, B.R., 2010. The value of estuarine and coastal ecosystem services. Ecol. Monogr. 81 (2), 169–193.

Bartholdy, J., 2000. Processes controlling import of fine-grained sediment to tidal areas: a simulation model. Geol. Soc. Lond., Spec. Publ. 175 (1), 13–29.

Bartholdy, J., Anthony, D., 1998. Tidal Dynamics and Seasonal Dependent Import and Export of Fine-grained Sediment Through a Back-barrier Tidal Channel of the Danish Wadden Sea, Tidal Sedimentology, Modern and Ancient. SEPM Special Publication pp. 43–52.

Brenner, O.T., Moore, L.J., Murray, A.B., 2015. The complex influences of back-barrier deposition, substrate slope and underlying stratigraphy in barrier island response to sea-level rise: insights from the Virginia Barrier Islands, Mid-Atlantic Bight, U.S.A. Geomorphology 246, 334–350.

Bruun, P., 1988. The Bruun rule of erosion: a discussion on large-scale two and three dimensional usage. J. Coast. Res. 4, 626–648.

Day, J.W., Christian, R.R., Boesch, D.M., Yanez-Arancibia, A., Morris, J., Twilley, R.R., Naylor, L., Schaffner, L., Stevenson, C., 2008. Consequences of climate change on the ecogeomorphology of coastal wetlands. Estuar. Coasts 31 (3), 477–491.

Emanuel, K.A., 2013. Downscaling CMIP5 climate models shows increased tropical cyclone activity over the 21st century. Proc. Natl. Acad. Sci. 110 (30), 12219–12224.

Feagin, R.A., Martinez, M.L., Mendoza-Gonzalez, G., Costanza, R., 2010. Salt Marsh Zonal Migration and Ecosystem Service Change in Response to Global Sea Level Rise: A Case Study From an Urban Region .

FitzGerald, D.M., Fenster, M.S., Argow, B.A., Buynevich, I.V., 2008. Coastal impacts due to sea-level rise. Annu. Rev. Earth Planet. Sci. 601–647 Annual Review of Earth and Planetary Sciences. Annual Reviews, Palo Alto.

Georgiou, I.Y., FitzGerald, D.M., Stone, G.W., 2005. The impact of physical processes along the Louisiana Coast. J. Coast. Res. 72–89.

Heinz-Center, 2000. The Hidden Costs of Coastal Hazards: Implications for Risk Assessment and Mitigation. Island Press.

IPCC, 2014. Climate Change 2014–Impacts, Adaptation and Vulnerability: Regional Aspects. Cambridge University Press.

Jiménez, J.A., Sánchez-Arcilla, A., 2004. A long-term (decadal scale) evolution model for microtidal barrier systems. Coast. Eng. 51 (8–9), 749–764.

Kirwan, M.L., Walters, D.C., Reay, W.G., Carr, J.A., 2016. Sea level driven marsh expansion in a coupled model of marsh erosion and migration. Geophys. Res. Lett. 43 (9) (2016GL068507).

Leatherman, S.P., 1983. Barrier dynamics and landward migration with Holocene sea-level rise. Nature 301, 415–417 (3 February).

Lorenzo-Trueba, J., Ashton, A.D., 2014. Rollover, drowning, and discontinuous retreat: distinct modes of barrier response to sea-level rise arising from a simple morphodynamic model. J. Geophys. Res. Earth Surf. 119 (4) (2013JF002941).

Mariotti, G., Carr, J., 2014. Dual role of salt marsh retreat: long-term loss and short-term resilience. Water Resour. Res. 50 (4), 2963–2974.

Mariotti, G., Fagherazzi, S., 2013. Critical width of tidal flats triggers marsh collapse in the absence of sea-level rise. Proc. Natl. Acad. Sci. 110 (14), 5353–5356.

McLachlan, A., 1983. Sandy beach ecology — a review. In: McLachlan, A., Erasmus, T. (Eds.), Sandy Beaches as Ecosystems. Developments in Hydrobiology. Springer, Netherlands, pp. 321–380.

McNamara, D.E., Werner, B.T., 2008. Coupled barrier island-resort model: 1. Emergent instabilities induced by strong human-landscape interactions. J. Geophys. Res. 113 (F01016). http://dx.doi.org/10.1029/2007JF000840.

Moore, L.J., List, J.H., Williams, S.J., Stolper, D., 2010. Complexities in barrier island response to sea level rise: insights from numerical model experiments, North Carolina Outer Banks. J. Geophys. Res. 115 (F3), F03004.

Morris, J.T., Sundareshwar, P.V., Nietch, C.T., Kjerfve, B., Cahoon, D.R., 2002. Responses of coastal wetlands to rising sea level. Ecology 83 (10), 2869–2877.

Morton, R.A., 2008. National Assessment of Shoreline Change: Part 1: Historical Shoreline Changes and Associated Coastal Land Loss Along the US Gulf of Mexico. DIANE Publishing.

Mudd, S.M., Howell, S.M., Morris, J.T., 2009. Impact of dynamic feedbacks between sedimentation, sea-level rise, and biomass production on near-surface marsh stratigraphy and carbon accumulation. Estuar. Coast. Shelf Sci. 82 (3), 377–389.

Murray, A.B., 2003. Contrasting the goals, strategies, and predictions associated with simplified numerical models and detailed simulations. In: Iverson, R.M., Wilcock, P.R. (Eds.), Prediction in Geomorphology, AGU Geophysical Monograph 135. Washington, D.C., pp. 151–165.

NAP, 1995. Beach Nourishment and Protection. National Academies Press, Washington, D.C.

Pedersen, J.B.T., Bartholdy, J., 2006. Budgets for fine-grained sediment in the Danish Wadden Sea. Mar. Geol. 235 (1–4), 101–117.

Raabe, E.A., Stumpf, R.P., 2016. Expansion of tidal marsh in response to sea-level rise: Gulf Coast of Florida, USA. Estuar. Coasts 39 (1), 145–157.

Rodriguez, A.B., Fegley, S.R., Ridge, J.T., VanDusen, B.M., Anderson, N., 2013. Contribution of aeolian sand to backbarrier marsh sedimentation. Estuar. Coast. Shelf Sci. 117, 248–259.

Rogers, L.J., Moore, L.J., Goldstein, E.B., Hein, C.J., Lorenzo-Trueba, J., Ashton, A.D., 2015. Anthropogenic controls on overwash deposition: evidence and consequences. J. Geophys. Res. Earth Surf. 120 (12) (2015JF003634).

Stolper, D., List, J.H., Thieler, E.R., 2005. Simulating the evolution of coastal morphology and stratigraphy with a new morphological-behaviour model (GEOMBEST). Mar. Geol. 218 (1–4), 17–36.

Teal, J.M., Weishar, L., 2005. Ecological engineering, adaptive management, and restoration management in Delaware Bay salt marsh restoration. Ecol. Eng. 25 (3), 304–314.

Tebaldi, C., Strauss, B.H., Zervas, C.E., 2012. Modelling sea level rise impacts on storm surges along US coasts. Environ. Res. Lett. 7 (1), 014032.

Titus, J.G., Park, R.A., Leatherman, S.P., Weggel, J.R., Greene, M.S., Mausel, P.W., Brown, S., Gaunt, C., Trehan, M., Yohe, G., 1991. Greenhouse effect and sea level rise: the cost of holding back the sea. Coast. Manag. 19 (2), 171–204.

Trembanis, A.C., Pilkey, O.H., Valverde, H.R., 1999. Comparison of beach nourishment along the U.S. Atlantic, Great Lakes, Gulf of Mexico, and New England shorelines. Coast. Manag. 27 (4), 329–340.

Vogel, R.L., Kjerfve, B., Gardner, L.R., 1996. Inorganic sediment budget for the North Inlet salt marsh, South Carolina, U.S.A. Mangrove Salt Marshes 1 (1), 23–35.

Walters, D.C., Kirwan, M.L., 2016. Optimal hurricane overwash thickness for maximizing marsh resilience to sea level rise. Ecol. Evol. 6 (9), 2948–2956.

Walters, D., Moore, L.J., Duran Vinent, O., Fagherazzi, S., Mariotti, G., 2014. Interactions between barrier islands and backbarrier marshes affect island system response to sea level rise: insights from a coupled model. J. Geophys. Res. Earth Surf (2014JF003091).

Weinstein, M.P., Teal, J.M., Balletto, J.H., Strait, K.A., 2001. Restoration principles emerging from one of the world's largest tidal marsh restoration projects. Wetl. Ecol. Manag. 9 (5), 387–407.

Wolters, M., Garbutt, A., Bakker, J.P., 2005. Salt-marsh restoration: evaluating the success of de-embankments in north-west Europe. Biol. Conserv. 123 (2), 249–268.